

CFD evaluation of a suitable site for a wind turbine on a trapezoid shaped hill

Thitipong Unchai^{*1} and Adun Janyalertadun²

¹Department of Physics, Faculty of Science, Ubonratchathani Rajabhat University, Thailand

²Department of Mechanical Engineering, Faculty of Engineering, Ubonratchathani University, Thailand

(Received April 7, 2012, Revised March 25, 2014, Accepted May 13, 2014)

Abstract. The computational fluid dynamic is used to explore new aspects of the hill flow. This analysis focuses on flow dependency and the comparison of results from measurements and simulations to show an optimization turbulent model and the possibility of replacing measurements with simulations. The first half of the paper investigates a suitable turbulence model for determining a suitable site for a wind turbine. Results of the standard k- ϵ model are compared precisely with the measurements taken in front of the hilltop. The Reynolds Stress Model showed exact results after 1.0 times of hill steepness but the standard k- ϵ model and standard k- ω model showed greater underestimation. In addition, velocity flow over Pha Taem hill topography and the reference geometry shape were compared to find a suitable site for a turbine in case the actual hill structure was associated with the trapezoid geometric shape. Further study of geometry shaped hills and suitable sites for wind turbines will be reported elsewhere.

Keywords: computational fluid dynamics; turbulent model; suitable site; wind turbine; trapezoid hill

1. Introduction

Global energy consumption has increased significantly in the last decade with the continued use of fossil fuels, which will eventually run out. The continued use of fossil fuels creates serious environmental problems, including acid emissions, air pollution and contributes to climate change. Many countries now provide renewable energy including solar, wave, geothermal and wind energy. Today, the use of wind energy technology has been developing very fast (Coelingh 1996, Sahin 1998, Vogiatzis 2004, Naif 2005, Al Nassar 2005), as wind power is a persistent local resource and is clean and environmentally friendly. The Energy Policy and Planning Office of Thailand (EPPO) showed electricity consumption for year 2009 was 134,729.89 GWh, of which 2,460.09 GWh were imported from neighboring countries. The cumulative electricity energy requirement has increased by an average of 10.5% and 39.9% from year 2005 and 1999, respectively. Thailand's energy resources are primarily crude oil, coal and natural gas. A report by EPPO showed, in December 31 2008, raw energy reserves were 183 MMBBL of crude oil and 12,003 BCF of natural gas (Department of Alternative Energy Development and Efficiency 2004). Therefore, wind

*Corresponding author, Ph. D., E-mail: thitipongunchai@gmail.com

^aAssociate Professor, E-mail: janyalertadun@hotmail.com

energy is an attractive alternative energy, which would reduce imported electrical energy and is environmentally friendly.

The Ubonratchathani province is on a plateau in southeastern of Thailand and covers an area of 16,112 square kilometers with a population of 1.8 million people. The average height above sea level is approximately 123 m. 51.07% of the region is farmland and 78% of electricity used is by households and agriculture (Department of Alternative Energy Development and Efficiency 2004).

Pha Taem national park is located at the eastern side of Ubonratchathani district, near the Khong River. Fig. 1 shows that the hill is 240 m high with a 20.06° slope. The terrain behind the hilltop is a 1.66° rockbound slope with few obstacles, while the front of the hill being farmland and a river. The hill structure is located perpendicular to one fourth of the wind impact direction.

Currently, computational fluid dynamics techniques are used worldwide to investigate suitable sites for turbines. The effects of surface roughness, wall function problems, turbulent model etc, was simulated to utilize most of the available energy from the wind (Takahashi 2002, Blocken 2007, Hargreaves 2007, Undheim 2005, Undheim 2003). The fluent commercial codes with turbulent models were used in this article because of their availability, well-developed interface and broad verification and validation.

The case chosen in this analysis was measured on March 11, 2011, between 9:00 – 11:00. The ambient mean temperature was 27.2°C and the mean pressure was 1009.43 pascals. The mean wind speed at the 10 m high reference station was 2.728 m/s and the direction was 2.4° vertical with 10.8° turning.

2. Turbulence model description

Turbulence of flow is difficult to define precisely, and is most often described by its properties. The first property of turbulence described by Panofsky and Dutton (Al Nassar 2005), states that the fluid velocity is a chaotic and apparently random function of both space and time. This means that the turbulence information is contained in the velocity fluctuations. The only expression containing the velocity fluctuations are the Reynolds stresses, which represent the turbulence of the flow. Another property of the turbulence is its non-linearity. The Reynolds stresses are also non-linear terms, in accordance with its property are contained within the Reynolds Averaged Navier-Stokes equations:

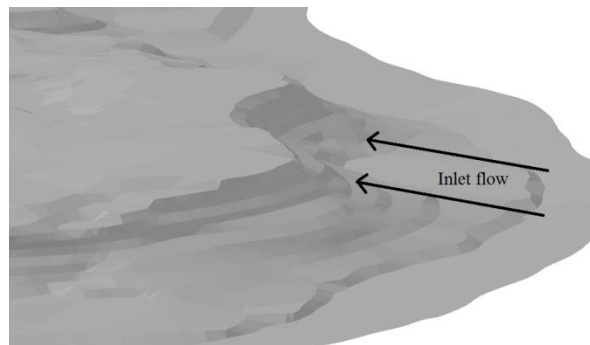


Fig. 1 Geographic Information System of geometry with a 1:50,000 resolutions

$$P \frac{\partial U_i}{\partial t} + U_j \frac{\partial U_i}{\partial x_j} = -\frac{1}{\rho} \frac{\partial p}{\partial x_i} - \frac{\partial \overline{U_i U_j}}{\partial x_j}, \quad (1)$$

$$\frac{\partial U_i}{\partial x_i} = 0 \quad (2)$$

where U_j are the Reynolds averaged components of the mean flow, P is the pressure, ρ is the density and $\overline{u_i u_j}$ with an over bar are turbulent stresses. This formulation includes both vertical and horizontal turbulent flux divergence. Equations for each of the six Reynolds stresses and dissipations are solved at each time step to close the mean equations. The model equations are solved using a fractional step method in which the equation for pressure is derived in such a way that it ensures a divergence-free momentum field.

The standard k- ε model is the industrial standard turbulence model in engineering practice. In this case, the transport equations of momentum, potential temperature, mixing ratio of water vapor and turbulence energy are adopted, while near-wall treatment are enhanced (Department of Alternative Energy Development and Efficiency 2004). Because of their computational robustness and efficiency, the two-equation k- ε turbulence model and its variants are most commonly used in wind energy research (The Ministry of Interior 2010, Feregh 1993). In particular, they have been extensively validated and calibrated for engineering application flows around bluff bodies and structures (Celik 2003).

2.1 k- ε model

The standard k- ε model (Launder 1972) is a semi-empirical model based on model transport equations for the turbulence kinetic energy (k) and its dissipation rate (ε). The model transport equation for k is derived from the exact equation, while the model transport equation for ε was obtained using physical reasoning and bears little resemblance to its mathematically exact counterpart.

In the derivation of the k- ε model, it was assumed that the flow is fully turbulent, and the effects of molecular viscosity are negligible. The standard k- ε model is therefore valid only for fully turbulent flows, so that

$$\mu_{eff} = \mu + \mu_t \quad (3)$$

where μ_t is the turbulence viscosity. The k- ε model assumes that the turbulence viscosity is linked to the turbulence kinetic energy and dissipation via the relation

$$\mu_t = C_\mu \rho \frac{k^2}{\varepsilon} \quad (4)$$

2.2 k- ω model

The standard k- ω model is an empirical model based on model transport equations for the

turbulence kinetic energy (k) and the specific dissipation rate (ω), which can also be thought of as the ratio of ε to k (Wilcox 1998).

One of the advantages of the k - ω formulation is the near wall treatment for low-Reynolds number computations. The model does not involve the complex non-linear damping functions required for the k - ε model and is therefore more accurate and more robust. A low-Reynolds k - ω model would typically require a near wall resolution of $y^+ < 0.2$, while a low-Reynolds number k - ε model would require at least $y^+ < 2$. In industrial flows, even $y^+ < 2$ cannot be guaranteed in most applications and for this reason; a new near-wall treatment was developed for the k - ω models. It allows for smooth shift from a low-Reynolds number form to a wall function formulation.

The k - ω models assumes that the turbulence viscosity is linked to the turbulence kinetic energy and turbulent frequency via the relation

$$\mu_t = \rho \frac{k}{\omega} \quad (5)$$

2.3 Reynolds stress model

The Reynolds stress model (Gibson 1978, Launder 1989, Launder 1975) involves calculation of the individual Reynolds stresses, $\overline{u_i u_j}$, using differential transport equations. The individual Reynolds stresses are then used to obtain closure of the Reynolds-averaged momentum equation

$$\frac{\partial}{\partial t}(\rho u_i) + \frac{\partial}{\partial x_i}(\rho u_i u_j) = -\frac{\partial p}{\partial x_i} + \frac{\partial}{\partial x_j} \left[\mu \left(\frac{\partial u_i}{\partial x_j} + \frac{\partial u_j}{\partial x_i} - \frac{2}{3} \delta_{ij} \frac{\partial u_l}{\partial x_l} \right) \right] + \frac{\partial}{\partial x_j} (-\rho \overline{u_i u_j}) \quad (6)$$

The exact form of the Reynolds stress transport equations may be derived by taking moments of the exact momentum equation. This is a process wherein the exact momentum equations are multiplied by a fluctuating property, the product then being Reynolds averaged. Unfortunately, several of the terms in the exact equation are unknown and modeling assumptions are required in order to close the equations. In this section, the Reynolds stress transport equations are presented together with the modeling assumptions required to attain closure.

3. Simulation

3.1 Experimental basis

Pha Taem national park is located at the eastern side of Ubonratchathani province, 500 m from the Khong River. The hill is 240m high from the bottom with a 20 degree slope. The wind data for this analysis was measured to enable comparison with the simulation data. The ambient mean temperature was 27.2°C and the mean pressure was 1009.43 pascal. The mean wind speed at the 10m high reference station was 2.728 m/s and direction was 2.4° with 10.8° turning.

Cup anemometer and wind vane with 0.1 m/s and 1.0° accreted were used to measure wind speed and direction at a height of 10m respectively. The measurement sites in front of the hill top were at -1.0 and -1.5 times that of the front-hill distance, while behind the hill top measurements

were taken at 0.0, 0.5, 1.0, 1.5 and 2.0 times that of the front-hill distance.

3.2 Grid arrangements and boundary conditions

The three different grids described in Table 1 were used to test the grid dependence to investigate the first grid cell enlargement of this work. The three grids cell size domains are called coarse, medium and fine with an increasing rate of 8%, 10% and 12% being analyzed.

The calculated figure of '5.9' shows that the separation point sensitivity to the thickness of the first cell is huge.

Generally, the medium grid gave almost the same result as the fine grid, but the extra computational effort of the fine grid was considerable. The coarse grid lost some details, and the separation and the reattachment point had a larger grid dependency.

Fig. 2 illustrates how the three grids used in the simulations highly influenced the results. Both the grid resolution and accuracy of the terrain data are important. The simulation domain is chosen to include the neighboring hills behind the Pha Taem hill, and the grid used in the simulations has a horizontal extension of 1 km in front of the hilltop, to 1 km behind the hilltop. The width of the domain is about 1 km, and the height of the domain is 1 km. The horizontal and vertical distribution of the grid cells is visualized in Figs. 3(a) and 3(b), respectively. The resolution in the center is $\Delta x = 1.0$ m and $\Delta y = 1.0$ m. This is constant in a central square of 500 m x 500 m, with a linear increase of 11% in the x-direction and 9% in the y-direction outside this square. The largest cell is 109.53 m in the x-direction and 27.69 m in the y-direction. The height of the first grid cell is $\Delta z = 1.0$ m. With a vertical stretching of 10%, the largest vertical extension is 108.54 m. The total amount of grid cells is 590x564x45.

A one-dimensional simulation was conducted to establish a profile over homogeneous conditions. With the roughness length $z_0=0.04$ m, the simulated velocity 10 m above ground level becomes 2.728 m/s. This profile is used as a whole inflow boundary condition and the initial condition for the entire domain. At the side boundaries, there are periodic boundary conditions, and at the outflow boundary there is a zero-gradient condition. The surface boundary condition is expressed by wall functions, connecting the velocity in the first cell to the roughness and the log law assumption. The top boundary is a zero-gradient surface in all variables except the vertical velocity, which is defined not to allow any material transports through the boundary. This means a vertical velocity equal to zero at the top boundary.

Table 1 Essential sizes of the grid dependence test

Properties	Coarse	Medium	Fine
Dimension	2,000×1,000	2,000×1,000	2,000×1,000
First grid cell size (m)	0.25493	0.04181	0.00709
Increasing rate	8%	10%	12%
Largest cell size (m)	70.20	85.64	96.59

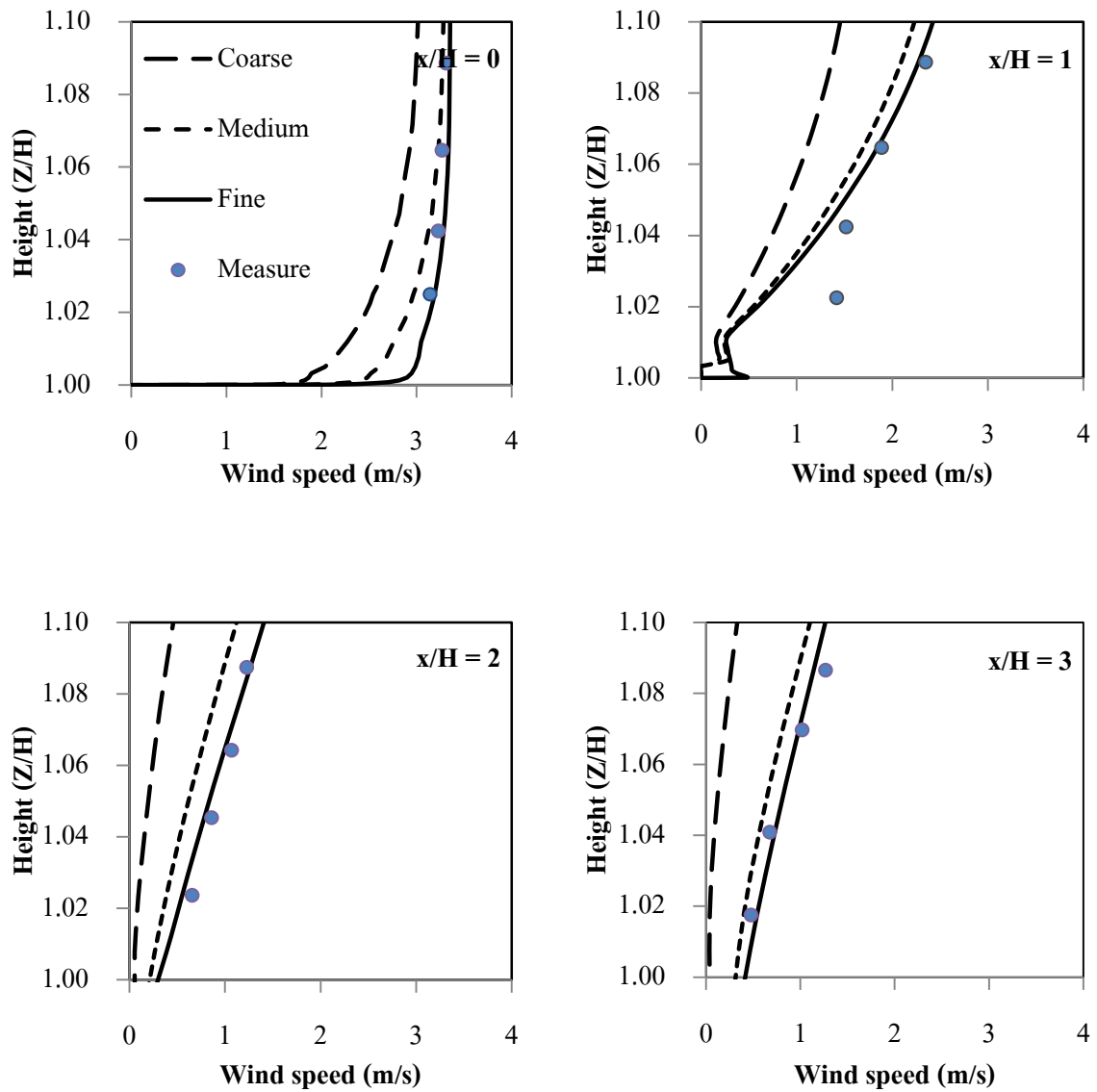


Fig. 2 Grid resolution sensitivity

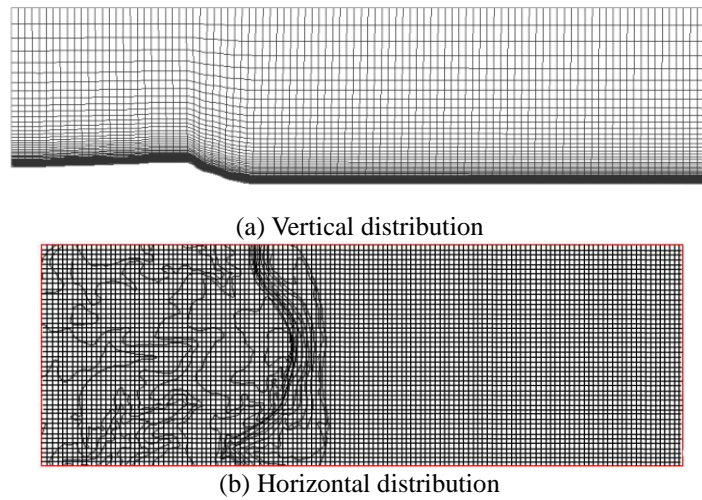


Fig. 3 Distribution of grids cells used in the simulations

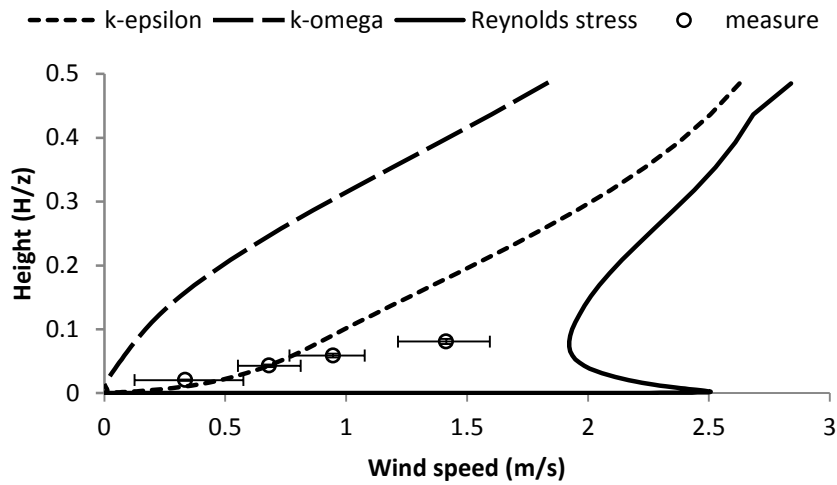


Fig. 4 Wind velocity profile at reference station

4. Results

4.1 General results

Fig. 4 showed the comparison of wind profiles at the reference station from standard $k-\epsilon$ model, standard $k-\omega$ model, RSM, and measurements, which were compared at the vertical velocity along -1.0 time of front hill, distance in front of the hill top. The simulations and measurements were

compared at 5 m, 10 m, 15 m and 20 m heights. The comparison showed the measurements were related to the standard $k-\epsilon$ model. Since, some results data from the standard $k-\epsilon$ model were in uncertainty range of the measurements, while the trend lines of standard $k-\omega$ model and RSM was dissimilar. The standard $k-\epsilon$ model has been shown to be useful for free-shear layer flows with relatively small pressure gradients. Similarly, for wall-bounded and internal flows, the model gives good results only in cases where mean pressure gradients are small; accuracy has been shown experimentally to be reduced for flows containing large adverse pressure gradients.

4.2 Comparison of velocity

The horizontal velocity comparison showed increased velocity in RSM while $k-\epsilon$ model and $k-\omega$ model showed similar results. Fig.5 highlights the velocity increase of each model of RSM, $k-\epsilon$ model and $k-\omega$ model occurred 16.45%, 8.42% and 7.76%, respectively. In addition, the maximum velocity in simulation appeared in turn at 2.36, 2.11 and 1.73 times of hill height is shown.

Fig. 6 shows the comparison of the measured and the simulated velocity and uncertainty limits at 10 m height from the ground. The results are separated in three phases. In the initial phase the standard $k-\epsilon$ model showed similar results with the measured results. In the second phase, along hilltop to 1.0 times of hill slope, the simulation results showed that the standard $k-\epsilon$ model and standard $k-\omega$ model was underestimated while RSM showed an overestimation. The final phase after 1.0 times of hill slope, the RSM showed exact results but the standard $k-\epsilon$ model and standard $k-\omega$ model showed more underestimation. This is because RSM naturally include the effects of streamline curvature, sudden changes in the strain rate, secondary flows or buoyancy compared to turbulence models using the eddy-viscosity approximation.

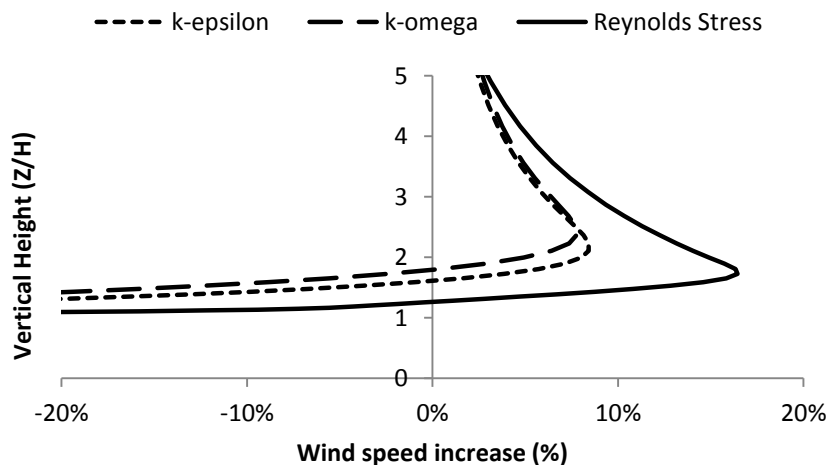


Fig. 5 Comparison of increasing speed at the hill top

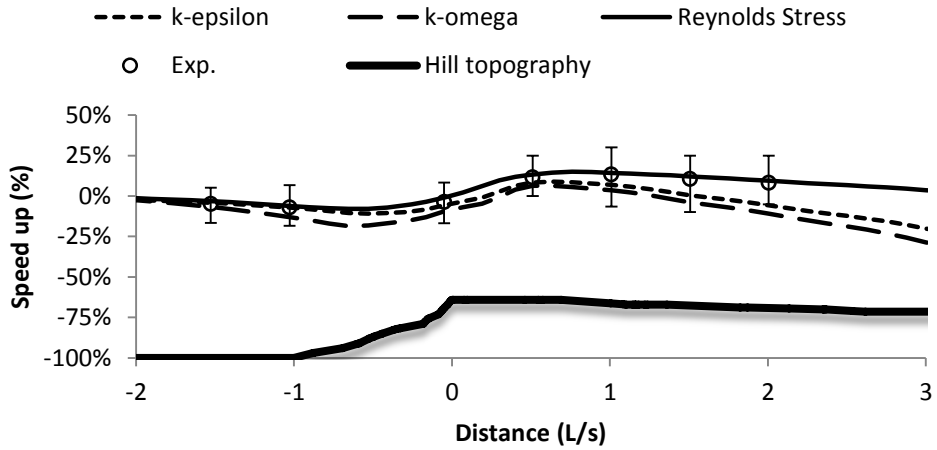


Fig. 6 Comparison of velocity at 10 m height from ground along the hill

4.3 Comparison of turbulence kinetic energy

Fig. 7 illustrates a comparison of measured and simulated results for turbulence kinetic energy along wind direction. The k-ε model showed greater convergence with the measured results than the earlier to distance 0.5 L/s after impact, while RSM and k-ω model expression was more appropriate. After the distance 0.5 L/s the complete simulation appeared as an underestimation of TKE at a height of 10 m.

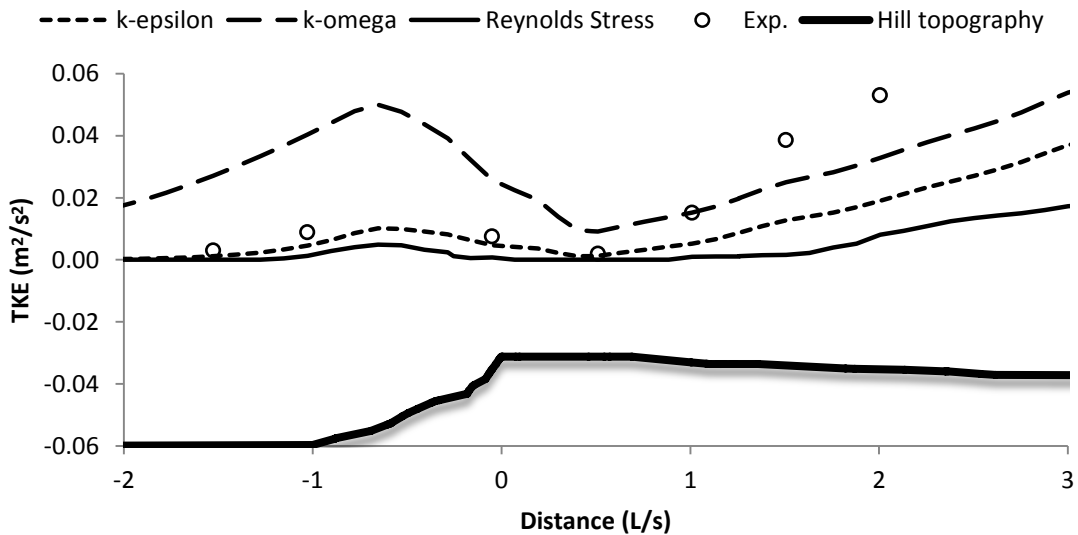


Fig. 7 Comparison of turbulence kinetic energy along wind direction at 10 m height

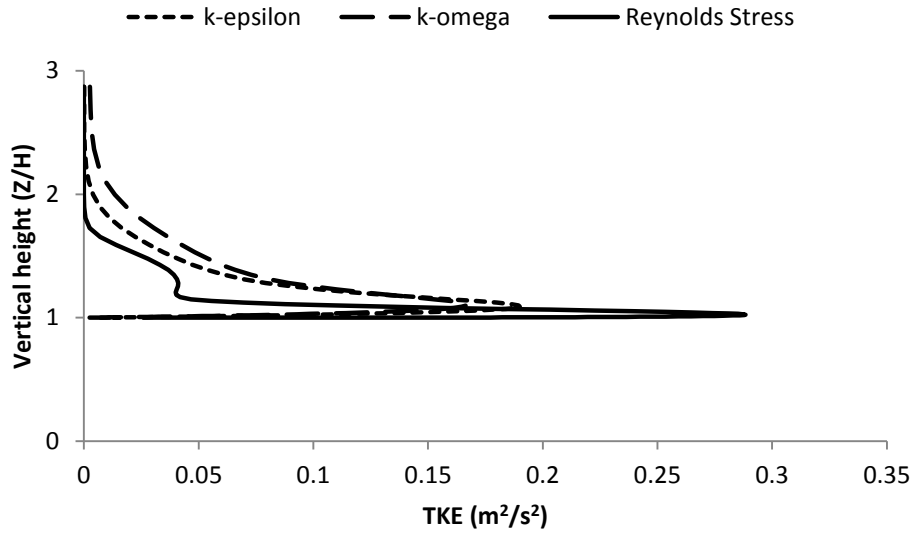


Fig. 8 Comparison of turbulence kinetic energy at distance 0.5 L/s

Through turbulence kinetic energy, shows kinetic energy of mass, received from root mean square of Eddies current. Fig. 8 shows the turbulence kinetic energy at a distance of 0.5 L/s, its maximum peak was at a little height from the flat terrain, but RSM greatly overestimated at ground level. On the other hand, the k-ε model and k-ω model showed underestimated with a wide gap. The peak value of turbulence kinetic energy for the RSM, k-ε model and k-ω model appeared 0.288, 0.190 and 0.166 m²/s², respectively.

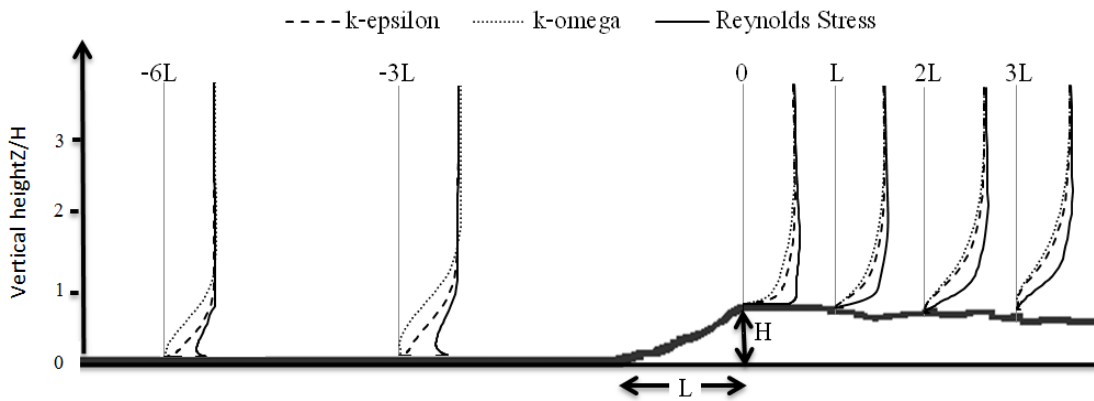


Fig. 9 Mean velocity component in the longitudinal direction

4.4 Mean velocity component in the longitudinal

Velocity profiles are used to investigate suitable sites for turbines; hill height H and slope distance L are implied procedures. Simulations were made at difference distances along the hill from $-6L$ to $3L$ for two cases, that is, inflow profile before impact ($-6L$ and $-3L$) and velocity profile after impact ($0L$ to $3L$). The mean velocities in a vertical direction around the hill are shown in Fig. 9. The inlet profile flow from $-6L$ to $-3L$ is steady, illustrating that the profile model is appropriate. After the impact line ($0L$) the simulation showed the velocity profiles change along the distance. The results from RSM indicated greater velocity than $k-\epsilon$ model and $k-\omega$ model along the ground to 2 times the hill height, while $k-\epsilon$ model and $k-\omega$ model demonstrated rather similar results.

5. Comparison of hill shape and geometry shape

The Pha Taem hill topography is quite similar to the geometry. To investigate a suitable site for wind turbines matching with real topography, reference geometry shapes are used to associate with the actual hill structure as shown in Fig.10. The hill shape can be separated into two parts, the hill with 20.06° slope and the flat rocky plate with a 1.66° slope to the backside with a few fences. The trapezoid geometry with a 20.0° slope and the flat plate 1.7° slopes to the backside with 0.04m roughness is used to examine this case.

Fig. 11 showed increasing velocity at $0.5 L/s$ from the hilltop. The RSM simulations indicated that resulted from Pha Taem hill topography provide similar velocities with the reference geometry shape from ground to $2 Z/H$ in vertical height, but in higher region the RSM showed further resulted at 2.63% in this region. The simulations from $k-\epsilon$ model and $k-\omega$ model illustrated similar tendency, which Pha Taem hill topography appeared additional results at 5.02% and 10.53% , since, the rocky plate roughness surface from topography compose more turbulent intensity.

Investigation of the turbulence kinetic energy, comparison of the flow over PhaTaem hill topography and reference geometry shape are shown in Fig. 12. The simulation results from $k-\omega$ model showed mostly similar results with a 2.97% difference, while the $k-\epsilon$ model showed an 8.02% difference. The RSM results demonstrated a twofold increase of turbulence kinetic energy.

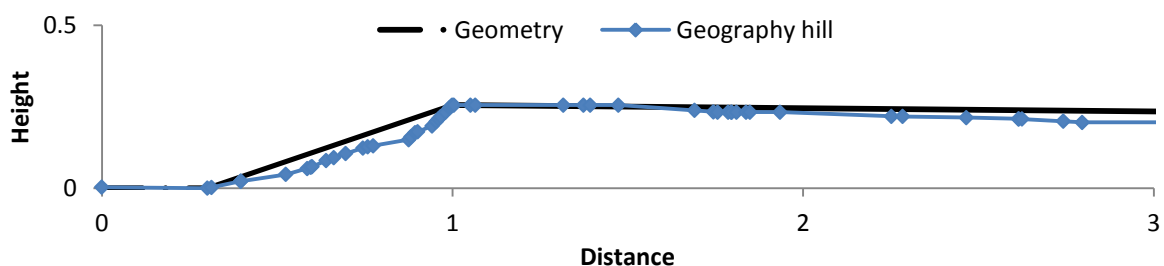


Fig. 10 Pha Taem topography associate with reference trapezoid geometry

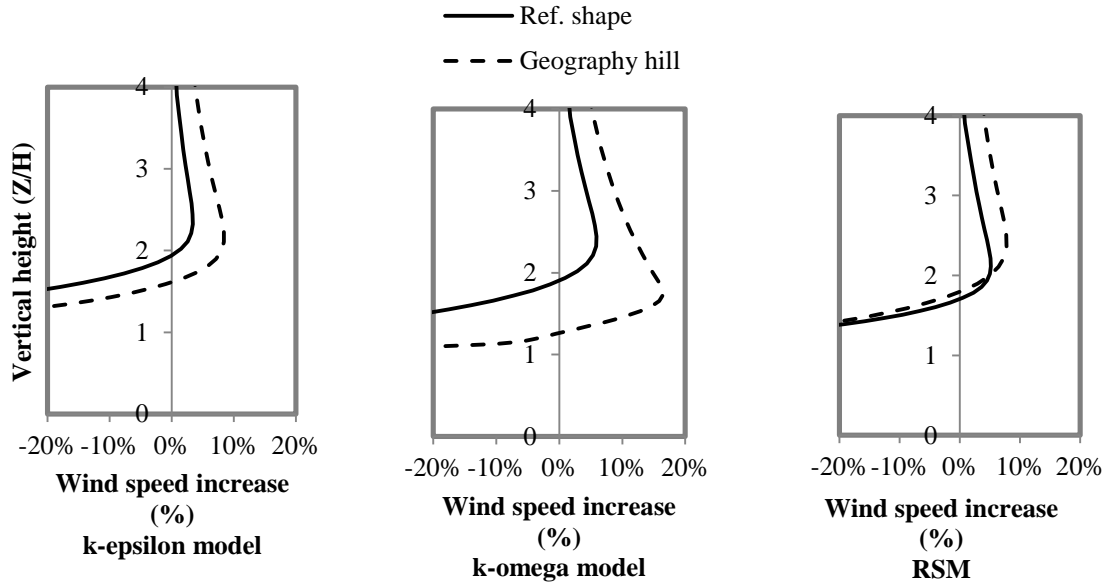


Fig. 11 Increase of velocity comparison of Pha Taem hill topography and reference geometry shape

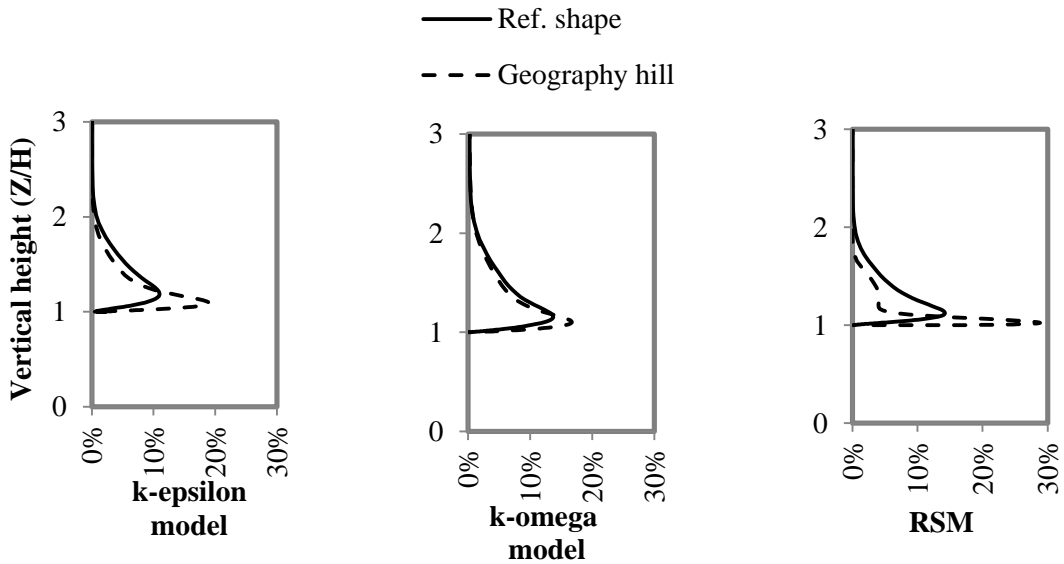


Fig. 12 Comparison of turbulence kinetic energy increasing of the flow over Pha Taem hill topography and reference geometry shape

6. Conclusions

Computational fluid dynamics is used to analyze the Pha Taem hill flow where the hill shape can be separated into two parts, the hill with 20.06° slope and the flat rocky plate with 1.66° slopes to backside and a few fences. The standard k- ϵ model, standard k- ω model and RSM were used to compare with measurements. Wind speed and direction, pressure and temperature were collected at 5 m, 10 m, 15 m and 20 m height for 7 stations.

The mean wind velocity at 10m height on measured date was 2.728 m/s, the wind velocity at 40m height was 3.014 m/s. Investigation of measured and the simulated wind velocity, and uncertainty limits at 10 m height from ground were made. The results illustrate that the standard k- ϵ model showed similar results to the measurements taken in front of the hilltop. After 1.0 times of hill slope the RSM showed exactly the same results, however, the standard k- ϵ model and standard k- ω model showed an underestimation. The turbulence kinetic energy in the simulations proved the standard k- ϵ model showed great alignment with the measured results at a distance of 0.5 L/s after impact, at a greater distance than 0.5 L/s the complete simulation appeared as an underestimation of TKE at 10 m height.

Comparison of the Pha Taem hill topography which is similar to trapezoid geometry with a 20.00° slope and the flat plate 1.7° slope to the backside with 0.04 m roughness. The coefficient of determination of Pha Taem hill and trapezoid is 0.9546. The RSM simulations indicated that resulted from Pha Taem hill provide similar velocity with trapezoid from ground to 2 Z/H in vertical height, but in higher regions the RSM showed results at 2.63% in this region. Investigation of the turbulence kinetic energy, the k- ω model showed most similarity with the measured results, corresponding with the turbulence intensity trend.

Reference

- Al Nassar, W., Alhajraf, S., Al-Enizi, A. and Al-Awadhi, L. (2005), "Potential wind power generation in the State of Kuwait", *Renew Energ.*, **30**(14), 2149-2161.
- Blocken, B. (2007), "CFD simulation of the atmospheric boundary layer: wall function problems", *Atmos. Environ.*, **41**(2), 238-252.
- Celik, A.N. (2003), "A statistical analysis of wind power density based on the Weibull and Rayleigh models at the southern region of Turkey", *Renew. Energ.*, **29**(4), 593-604.
- Coelingh, J.P., Van Wijk, A.J.M. and Holtslag, A.A.M. (1996), "Analysis of wind speed observation over the North Sea", *J. Wind Eng. Ind. Aerod.*, **61**(1), 51-69.
- Department of Alternative Energy Development and Efficiency, Ministry of Energy, Thailand (2004), <http://www.eppo.go.th/index-E.html>, Access on 12 Dec 2011.
- Feregh, G.M. (1993), "Wind energy potential for Bahrain", *Energy Convers. Manage*, **34**(6), 499-506.
- Gibson, M.M. and Launder, B.E. (1978), "Ground ejects on pressure fluctuations in the atmospheric boundary layer", *J. Fluid Mech.*, **86**, 491- 511.
- Hargreaves, D.M. and Wright, N.G. (2007), "On the use of the k- ϵ model in commercial CFD software to model the neutral atmospheric boundary layer", *J. Wind Eng. Ind. Aerod.*, **95**(5), 355-369.
- Launder, B.E. (1989), "Second-moment closure", *Int. J. Heat Fluid Fl.*, **10**(4), 282-300.
- Launder, B.E., Reece, G.J. and Rodi, W. (1975), "Progress in the development of a reynolds-stress turbulence closure", *J. Fluid Mech.*, **68**(3), 537-566.
- Launder, B.E. and Spalding, D.B. (1972), *Lectures in mathematical models of turbulence*, Academic Press, London, England.

- Ministry of Interior (2010), http://www.dopa.go.th/stat/y_stat.html. Access on 5 Nov 2011.
- Naif, M.Al-Abadi. (2005), "Wind energy resource assessment for five locations in Saudi Arabia", *Renew Energ.*, **30**(10), 1489-1499.
- Sahin, A.Z.Aksakal, A. (1998), "Wind power energy potential at the northeastern region of Saudi Arabia", *Renew Energ.*, **14**(1-4), 435-440.
- Takahashi, T., Ohtsua, T., Yassina, M.F., Kato, S. and Murakami, S. (2002), "Turbulence characteristics of wind over a hill with a rough surface", *J. Wind Eng. Ind. Aerod.*, **90**(12-15), 1697-1706.
- Undheim, O. (2003), "Comparison of turbulence models for wind evaluation in complex terrain", *Proceedings of the Conference EWEC 2003*.
- Undheim, O. (2005), "2D simulations of terrain effects on atmospheric flow", *Proceedings of the MekIT'05*.
- Vogiatzis, N., Kotti, K., Spanomitsios, S. and Stoukides, M. (2004), "Analysis of wind potential and characteristics in North Aegean Greece", *Renew Energ.*, **29**(7), 1193-208.
- Wilcox, D.C. (1998), *Turbulence modeling for CFD*, DCW Industries, Inc. La Canada, California.